Reduction of Myeloid-derived Suppressor Cells and Lymphoma Growth by a Natural Triterpenoid

Faisal F. Y. Radwan[1,2,3], **Azim Hossain**[1,2,3], **Jason M. God**[1,2,3], **Nathan Leaphart**[1,2,3], **Michelle Elvington**[1,2,3], **Mitzi Nagarkatti**[4], **Stephen Tomlinson**[1,2,3,§], and **Azizul Haque**[1,2,3,*]

[1]Department of Microbiology and Immunology, Medical University of South Carolina, 173 Ashley Avenue, Charleston, SC 29425

[2]Hollings Cancer Center, Medical University of South Carolina, 173 Ashley Avenue, Charleston, SC 29425

[3]Children's Research Institute, Medical University of South Carolina, 173 Ashley Avenue, Charleston, SC 29425

[4]Dept. of Pathology, Microbiology and Immunology, University of South Carolina School of Medicine, 6439 Garner's Ferry Road, Columbia, SC29208

Abstract

Lymphoma is a potentially life threatening disease. The goal of this study was to investigate the therapeutic potential of a natural triterpenoid, Ganoderic acid A (GA-A) in controlling lymphoma growth both *in vitro* and *in vivo*. Here, we show that GA-A treatment induces caspase-dependent apoptotic cell death characterized by a dose-dependent increase in active caspases 9 and 3, up-regulation of pro-apoptotic BIM and BAX proteins, and a subsequent loss of mitochondrial membrane potential with release of cytochrome c. In addition to GA-A's anti-growth activity, we show that lower doses of GA-A enhance HLA class II-mediated antigen presentation and CD4+ T cell recognition of lymphoma *in vitro*. The therapeutic relevance of GA-A treatment was also tested *in vivo* using the EL4 syngeneic mouse model of metastatic lymphoma. GA-A-treatment significantly prolonged survival of EL4 challenged mice and decreased tumor metastasis to the liver, an outcome accompanied by a marked down-regulation of STAT3 phosphorylation, reduction myeloid-derived suppressor cells (MDSCs), and enhancement of cytotoxic CD8+ T cells in the host. Thus, GA-A not only selectively induces apoptosis in lymphoma cells, but also enhances cell-mediated immune responses by attenuating MDSCs, and elevating Ag presentation and T cell recognition. The demonstrated therapeutic benefit indicates that GA-A is a candidate for future drug design for the treatment of lymphoma.

*Corresponding author: Dr. Azizul Haque, Department of Microbiology and Immunology, Medical University of South Carolina, 173 Ashley Avenue, BSB-201, Charleston, SC 29425, USA. haque@musc.edu Tel: +1-843-792-9466; Fax: +1-843-792-2464.
§Ralph H. Johnson Veterans Affairs Medical Center, Charleston, SC

CONFLICTS OF INTEREST

The authors have no financial conflicts of interest.

INTRODUCTION

While current cancer therapeutics possess many desirable properties, new natural products capable of modulating proliferation and immunogenicity of cancer cells have become a keystone in the search for new treatment strategies. The most notable disadvantage of existing chemotherapy of lymphoid malignancies is the resistance of a small percentage of tumors to drug induced cytotoxicity, resulting in long-term ineffectiveness of treatment and ultimately disease relapse [Ocker and Hopfner, 2012; Souza et al., 2012]. Hence, by inducing an enhanced immune response against resistant tumor cells, immune-mediated clearance and long-term survival may be achieved. A key aspect of generating an immune response to B-cell lymphoma includes HLA class II-mediated antigen presentation to CD4+ T cells [Morkowski et al., 1995]. However, B-cell lymphomas are unable to optimally process antigens for their delivery to CD4+ T cells via HLA class II molecules, a crucial step that results in their escape from T cell immunity [Amria et al., 2008; Drenou et al., 2004; Hossain et al., 2011]. A large number of aggressive B-cell lymphomas also lack β2-microglobulin and are unable to deliver Ag to CD8+ T cells via the HLA class I pathway. Thus, activating the HLA class II pathway of immune recognition may help expand and maintain a small number of tumor-specific CD8+ T cells. In this study, we report that Ganoderic Acid-A (GA-A), a natural extract of a medicinal mushroom *Ganoderma lucidum* (Fig. 1A), has the potential to play a dual-role in a chemo- and immunotherapeutic regimen of human B-cell lymphoma.

Ganoderma has been used for centuries in Far East countries as a folk remedy for its antitumor and health promoting effects [Hsieh and Wu, 2011; Sliva, 2003]. Due to its presumed health benefits and apparent absence of side-effects, it has also been widely consumed as a dietary supplement by cancer patients [Hsieh and Wu, 2011]. The major constituents of *Ganoderma* include polysaccharides and triterpenes [Boh et al., 2007; Wubshet et al., 2012], and both components seem to have profound anti-proliferative activities [Chen et al., 2004; Kimura et al., 2002; Sadava et al., 2009]. Ganoderic acids (GAs) are one of major compounds with potent pharmacological activity found in G. lucidum and these compounds belong to the triterpenoids. It is widely believed that GA possesses numerous properties including anti-oxidant, anticancer, antiviral, and anti-platelet aggregation properties. Although crude GAs and their derivatives have been tested in many occasions [Jiang et al., 2008; Li et al., 2012; Liu et al., 2012; Wu et al., 2012; Yao et al., 2012], purified GA-A has not been investigated in details. The molecular formula of GA-A is $C_{30}H_{44}O_7$, and its approximate molecular mass is 516 daltons. This natural product may have a potential to play important roles in immune regulation and inhibition of leukemia and lymphoma growth. The affordability of GA-A may also provide windows of opportunity, such as its co-administration with traditional anticancer drugs for overcoming cancer cell resistance to chemotherapy.

B-cell lymphoma arises in lymphoid organs due to unprecedented atypical proliferation of lymphoid cells, thus compromising immune function [Siegel et al., 2012]. The disease is regarded as a leading cause of new cancer cases in the United States. Recently, it has been estimated that leukemia and lymphoma accounts for 7.7% of new cancer cases and 7.6% of new cancer-related deaths in the US. B-cell lymphoma also occurs at any age, and the development and progression of this malignancy involves complex interactions between the neoplastic B-cells and the surrounding microenvironment, highlighting the need for a new therapeutic strategy. Recent studies suggest that myeloid-derived suppressor cells (MDSCs) represent a subset of antigen presenting cells which accumulate in tumor microenvironment and induce immune tolerance in malignancies [Goh et al., 2013; Kennedy et al., 2011; Khaled et al., 2013]. MDSCs are comprised of hematopoietic progenitor cells and precursors of macrophages, dendritic cells, and immature granulocytes. These cells are of great interest because they have the capacity to suppress the adaptive immune response mediated by both CD4$^+$ and CD8$^+$ T cells, promoting tumor growth and metastasis. [Mougiakakos et al., 2013; Srivastava et al., 2012b]. It remains unclear whether GA-A causes any alterations of MDSCs in lymphomas and negatively influences immune recognition. Regulatory T cells (Tregs) also play an essential role in the immunosuppressive networks that contribute to tumor-immune evasion [Facciabene et al., 2012]. In this study, we investigated both the *in vitro* and *in vivo* efficacy of GA-A treatment in controlling the growth of B-cell lymphoma. Our *in vitro* findings suggest that GA-A induces apoptosis in human B-cell lymphomas, and that equal concentrations of GA-A are less toxic to healthy primary B-cells and B-lymphoblastoid cell lines. We also show that GA-A treatment enhances CD4+ T cell recognition of lymphoma cells. Our *in vivo* data show that GA-A treatment reduces tumor load by simultaneous killing of lymphoma cells and enhanced immune recognition via reduction of MDSCs and activation of cytotoxic CD8+ T cells in the host.

MATERIALS AND METHODS

CELL LINES AND PRIMARY TUMORS

Human pre-B acute lymphocytic leukemia (NALM-6), Burkitt lymphoma (Ramos, GA-10, CA-46 and Daudi) and non-Hodgkin's lymphoma (Toledo and DB) cell lines were maintained as described previously [Amria et al., 2008; God et al., 2014; Radwan et al., 2012]. The Human Epstein-Barr virus (EBV)-transformed B-lymphoblastoid cell lines (B-LCL): 6.16, Frev and Priess were cultured in complete IMDM media as described [Hossain et al., 2012]. CA-46, GA-10, Toledo, and DB cell lines were purchased from American Type Culture Collection (ATCC St. Louis, MO). NALM-6, Ramos, Daudi, and 6.16 cells [Amria et al., 2008; Radwan et al., 2012] were obtained from Dr. Janice Blum (Indiana University), and were transduced using retroviral vectors for constitutive expression of HLA-DR4 (DRB1-0401) with linked drug selection markers for hygromycin and histidinol resistance [Haque et al., 2001; Hiraiwa et al., 1990; Kovats et al., 1995; Radwan et al., 2012]. Expression of surface HLA-DR4 complexes on cells was confirmed by flow cytometric analysis using the HLA-DR4-specific mAb, 359-F10 [Hiraiwa et al., 1990; Radwan et al., 2012]. The 6.16.DR4 cells were further transduced using retroviral vectors for constitutive expression of HLA-DM molecules [Haque et al., 2001; Kovats et al., 1995]. The expression of HLA-DM molecules on 6.16.DR4.DM cells was confirmed by western blotting. The T

cell hybridoma line 17.9, which responds to human serum albumin (HSA) residue 64–76K, and the human IgGκ$_{188–203}$ specific T cell hybridoma line 2.18a were maintained in complete RPMI-1640 media [Haque et al., 2002; Zhao et al., 2011]. Primary tumors including follicular B-cell lymphomas (TB#2759), diffuse large B-cell lymphoma (TB#2952) and chronic lymphocytic lymphoma (TB#3284) were obtained from Hollings Cancer Center, MUSC. The PI has an approved protocol (HR#17159) from the Institutional Review Board (IRB) of Medical University of South Carolina for this study. All the participants provided their written consent to participate in this study, which were approved by the IRB. Primary B-cells were separated from a healthy volunteer blood sample using EasySep® human naive B-cell enrichment kit (STEMCELL Technologies Inc., Vancouver, Canada) per manufacturer's instructions.

ANTIGENS, PEPTIDES AND ANTIBODIES

The human HSA$_{64–76K}$ peptide (VKLVNEVTEFAKTK) was produced using Fmoc technology and an Applied Biosystems Synthesizer as described [Haque et al., 2001; Hossain et al., 2011; Zhao et al., 2011]. The primary antibodies used were human caspase 8 (12F5) and caspase 3 (31A1067) (Alexis Biochemicals, Plymouth Meeting, PA); caspase 9 (ICE-LAP6, Mch6) and cytochrome c (136F3) (Cell Signaling technologies, Danvers, MA); APAF-1 (2E10), BCL-2 (C-2), BAX (B-9), BIM (H-191), survivin, Ii, HLA-DM, HLA-DR, STAT3 and p-STAT3 (Santa Cruz Biotechnology Inc., Santa Cruz, CA); and β-actin (clone AC-15) (Sigma Chemical Co., St. Louis, MO). Caspase 9, cytochrome c, BCL-2 and survivin antibodies were obtained from Drs. L. Xiang, J. Norris, and O. Moussa (Medical University of South Carolina). The secondary antibodies used were horseradish peroxidase conjugated anti-mouse (Pierce, Rockford, IL, USA), anti-rabbit or anti-goat IgG (Santa Cruz).

GANODERIC ACID A

Ganoderic Acid A (GA-A, Fig. 1A) has been isolated from the *Ganoderma lucidum* mushroom, and was purchased from Apin Chemicals Ltd, UK (Cat# 5058g). The purity (>98%) of GA-A was determined by the vendor using LC/MS analysis. GA-A was reconstituted in DMSO (Fisher Scientific) to make a 10mM stock solution for use in the cell viability assay. For all *in vitro* GA-A treatments, the final DMSO concentrations did not exceed 0.01% (v/v).

CELLULAR VIABILITY ASSAYS

Cells were seeded at 1×10^4 cells/well in 100μl of appropriate culture medium in a flat-bottom 96-well plate. GA-A was added to appropriate wells for final concentrations of 5, 10, 20, and 40μM. Following 24h of GA-A treatment, cell viability was measured using the CellTiter 96 AQueous One Solution Cell Proliferation Assay (MTS; Promega, Madison, WI) [Hossain et al., 2012; Radwan et al., 2012]. Data are representative of at least three separate experiments and are expressed as cell viability (% of control) ± S.D. of triplicate wells.

To estimate cell death in lymphoma-patient primary B-cells, non-viable cells in treated and control batches were counted by trypan blue dye exclusion, and the percent cell death was calculated [Hossain et al., 2012]. Doses up to 80μM of GA-A were used to estimate IC$_{50}$

values, which were analyzed using nonlinear regression analysis and a sigmoidal dose-response equation (GraphPad Prism). Experiments were repeated at least three times and the data are expressed as percent cell death ± S.D. of triplicate wells.

CASPASE ACTIVATION AND INHIBITION ASSAYS

Lymphoma cells were treated with different concentrations of GA-A, and subjected to a subsequent assay for cellular activity of caspase(s). Briefly, 5×10^4 cells were plated in 100μl of total volume in a 96-well plate and treated with 20μM of GA-A for 24h at 37°C. The plate was then equilibrated for 30 min at room temperature and 100μl of Caspase-Glo® 9 or 3/7 reagents (Promega Corporation, Madison, WI) was added to each well. Luminescence was recorded 30 min after adding reagents using a Floustar Optima microplate reader (BMG, Durham, NC) as described[Hossain et al., 2012]. To further analyze caspase activity, cells were treated with GA-A (5, 10, 20, or 40μM) in the presence or absence of the pan-caspase inhibitor Z-VAD-FMK at a 50 μM final concentration (R&D systems #FMK001). Cells treated with vehicle alone were used as controls. Cells were then incubated at 37°C for 24h, and cell viability was measured using the MTS assay as described [Radwan et al., 2012].

STAINING WITH ANNEXIN V AND TMRE

Cells treated with vehicle alone or GA-A (20μM) were stained with Annexin V-FITC and propidium iodide (PI) as described [Hossain et al., 2012]. To examine mitochondrial dysfunction which may contribute to cytochrome c release, cells treated with vehicle alone or GA-A (20μM) were stained with TMRE (tetramethylrhodamine ethyl ester, 200nM) (Sigma), and analyzed by flow cytometry according to the manufacturer's protocol [Hossain et al., 2012]. Triplicate samples were analyzed by a FACScan flow cytometer using CellQuest software (BD Bioscience, Mountain View, CA).

CYTOPLASMIC AND NUCLEAR FRACTIONATION

Cells treated with GA-A (20μM) or vehicle alone were incubated for 24h, washed once in Dulbecco's phosphate-buffered saline and fractionated as described previously [Surjit et al., 2005]. Briefly, cells (1×10^7) were resuspended in 200μl of ice cold buffer A (10mM HEPES, pH 7.9, 0.1mM EDTA, 0.1mM EGTA, 1 mM dithiothreitol, protease inhibitor cocktail) for 15 min on ice, followed by the addition of 15μl of 10% NP-40 and vortexed vigorously for 10 seconds. The samples were first spun at 4,500×g for 1 min, to pellet nuclei (as confirmed under microscopy). The supernatant was clarified again at 9,300×g for 10 min, and used as a cytoplasmic fraction for subsequent western blot analysis for the detection of APAF-1 and cytochrome c proteins.

WESTERN BLOT ANALYSIS

Cells were cultured for 24h in the presence GA-A (5, 10 and 20μM) or vehicle alone and subjected to western blot analysis [Hossain et al., 2012]. The blots were probed with antibodies for the detection of caspases (3, 8 and 9), cytochrome c, APAF-1, survivin, BCL-2, BAX, BIM and HLA-DR according to manufacturer's instructions. Samples (liver and spleen) obtained from vehicle and GA-A-treated EL4-bearing mice were also analyzed by western blotting for STAT3 [(C-20): sc-482] and p-STAT3 [(Tyr 705): sc-7993] proteins.

β-actin was used as a protein loading control. Relative protein expression was also assessed using a Bio-Rad scanning densitometer and further stated as a ratio of specific proteins expressed/β-actin for each sample [Goldstein et al., 2008; Radwan et al., 2012; Zhao et al., 2011].

FLOW CYTOMETRIC ANALYSIS

Treated and control cells (20μM of GA-A, or vehicle alone) were stained with the HLA-DR4-specific antibody (359-F10), followed by a Fluorescein isothiocyanate (FITC)-labeled secondary antibody (anti-rat IgG, Santa Cruz) [Haque et al., 2007; Hiraiwa et al., 1990; Zhao et al., 2011]. Background fluorescence was evaluated using irrelevant isotype-matched mAbs IN-1 [Hossain et al., 2011; Zhao et al., 2011]. After subtracting nonspecific background, the mean fluorescence Intensity (MFI) was used to compare the relative protein expression on the cell surface in treated and control cells. The expression of MHC (class I and class II) and co-stimulatory molecules (CD80, CD86) on cell surface of spleen cells obtained from GA-A treated and control mice was also analyzed. Briefly, spleen cells (1×10^6) of GA-A treated (Group 1), untreated (Group II), and control (Group III) were incubated with FITC-conjugated anti-mouse MHC class I (H-2D^d), anti-mouse class II (I-A/I-E), anti-mouse CD80, and anti-mouse CD86 antibodies (Santa Cruz). Intracellular staining of pooled lymph node/spleen cells with Foxp3-PE, CD4-PerCP, Gr-1-FITC and CD11b-PE (Santa Cruz) was also performed using a standardized protocol. Appropriately conjugated, isotype-matched IgGs served as controls. After staining, flow cytometric analysis was performed for three independent assays using a FACScan with CellQuest software (BD Bioscience, Mountain View, CA).

To determine serum IgG and/or IgM levels, EL4 cells (1×10^6 in 1ml PBS) were incubated with sera obtained from vehicle alone or GA-A treated mice for 30 min, washed, and incubated with 10μl of FITC-conjugated mouse anti-IgG or anti-IgM antibodies (Bethyl Laboratories, Montgomery, TX, USA) for 10 min. Cells were washed again, and fixed with 1% para-formaldehyde before being analyzed by flow cytometer.

To analyze IFN-γ producing CD8+ T cells, spleen cells from vehicle and GA-A-treated mice (pooled, n=3) were treated with 75 ng/ml of PMA plus 300 ng/ml of ionomycin, and stained with PE-labeled rat anti-mouse CD8 monoclonal antibody [BD Pharmingen (clone 53–6.7, Cat. No. 553033)]. After washing, the cells were fixed, permeabilized, and subsequently stained with FITC-labeled rat anti-mouse IFN-γ (Clone XMG1.2, Cat. No. 554411). Cells were then analyzed by flow cytometry.

ANTIGEN PRESENTATION ASSAYS

Cells (2×10^4 cells/well) were treated with either vehicle alone or 5, 10 or 20μM GA-A for 24h at 37°C in culture media in 96-well plate. To examine changes in cellular ability of presentation of exogenous antigens after treatment, the HSA or HSA$_{64–76K}$ peptide (10μM) was added to the appropriate wells for the last 4–6h of incubation. Cells were then washed and co-cultured with the HSA$_{64–76K}$ peptide specific T cell hybridoma (17.9) for 24h. The production of IL-2 in the culture supernatants was tested by ELISA [Haque et al., 2002; Radwan et al., 2012; Younger et al., 2008]. To test the changes in presentation of

endogenous antigens, Daudi.DR4 and Priess.DR4 cells (both express endogenous IgGκ) were treated with GA-A for 24h, washed and co-cultured with the human $IgG\kappa_{188-203}$ peptide specific T cell hybridoma (2.18a) for another 24h. T cell production of IL-2 was quantitated by ELISA as mentioned above [God et al., 2014; Radwan et al., 2012]. The amount of IL-2 in the culture supernatant corresponds to activation of CD4+ T cells. All assays were repeated at least three times.

GA-A TREATMENT REDUCES TUMOR METASTASIS IN EL4 LYMPHOMA MODEL

Male C57BL/6 mice (5 weeks old, 18–21g on average) were obtained from the Jackson laboratories. An EL4 tumor-bearing mouse model was established in mice as previously described [Imai et al., 2007; Knoepp et al., 2008]. The mice were housed under Specific Pathogen Free conditions (room temperature, $22 \pm 3°C$; humidity, 60%) with commonly available chow and tap water. Mouse T cell lymphoma line EL4 (1×10^5 cells in 100μl PBS) was injected i.v. into two groups of mice (Group 1, and Group II) (8 mice/group). A third group (Group III) containing 6 mice was used to represent sham control. Group I (GA-A treatment group) received a series of three i.p. doses of GA-A containing 60, 50 and 50mg/kg body weight at day 10, 14 and 18 after EL4 injection, respectively. The final concentration and volume of GA-A for i.p. injection was 1mg/50 μl of DMSO per mouse. Meanwhile, control groups (untreated and sham) received equivalent volumes (50μl per mouse) of vehicle solution. Tumor-bearing animals were sacrificed if they showed severe signs of moving disability that hamper them from obtaining food and water. Necropsies were done to scarified animals to examine the number of liver tumors, liver weight, and liver appearance [Knoepp et al., 2008]. All work with mice was approved by the Medical University of South Carolina Animal Protocols Review Board and was performed in accordance with the National Institutes of Health Guide for Care and Use of Laboratory Animals.

STATISTICAL ANALYSIS

Data from each experimental group were subjected to statistical analysis. Differences between experimental groups were analyzed for statistical significance using Student's t-test and analysis of variance (ANOVA) as appropriate. Values of P 0.05 were considered significant.

RESULTS

GA-A INDUCES ANTI-PROLIFERATIVE ACTIVITY IN B-CELL LYMPHOMAS

Screening of GA-A anti-proliferative effect was carried out simultaneously on several early passage human B-cell lymphoma and B-lymphoblastoid cell lines in addition to primary B-cell lymphoma and healthy B-cells obtained from lymphoma patients and healthy donors. GA-A treatment induced significant dose-dependent anti-proliferative activity (reduced viability) in all lymphoma cells tested, with a calculated IC_{50} ranging from 18.5 to 22μM in Burkitt's lymphomas (Fig. 1B), and about 15μM in non-Hodgkin's lymphomas (Fig. 1C). A significantly lower viability was detected in GA-A-treated B-lymphoblastoid cells, with an IC_{50} ranging from 32 to 45μM (Fig. 1D). It is notable that 40μM of GA-A caused a nearly 2-fold increase in reduction of viability in lymphoma cell lines (averaged 63.8±10.6 %)

compared to B-lymphoblastoid cell lines (37.6±1.5). In addition, similar anti-growth activity assays showed that GA-A elicited a notable 2-fold decrease in cell viability in primary tumors compared to normal healthy B-cells (Fig. 1E). Data from the 40μM GA-A treatment showed an average of 73.2±11.3% decrease in cell viability in primary B-cell lymphoma vs. 35.5±4.3% reduction in cell growth in healthy primary B-cells. Taken together, the above data demonstrate a preferential anti-proliferative activity of GA-A in B-lymphoma cell lines and primary tumors compared to B-cell lines and healthy primary B-cells.

GA-A INDUCES CASPASE-DEPENDENT APOPTOSIS

To study the mechanisms of GA-A-mediated anti-proliferative activity in human lymphomas, we focused on a known pre-B acute lymphocytic leukaemia line (NALM-6) and a B-lymphoblastoid cell line (6.16). Western blot analysis of treated cells showed the presence of cleaved caspase 3, 8, and 9 proteins, suggesting that GA-A mediates apoptotic cell death by the activation and processing of caspases into a number of catalytic subunits (Fig. 2A). GA-A-initiated cleavage of caspases followed a dose-dependent fashion, and a greater extent observed in NALM-6 cells compared to a B-cell line 6.16 which was less sensitive to GA-A (Fig. 2A). A significant increase in caspase catalytic activities of caspase 9 and 3/7 were also measured in NALM-6 cells after 24h of treatment with 20μM GA-A (Fig. 2B). A pan-caspase inhibitor Z-VAD-FMK, which is known to bind to the catalytic site of caspases, almost completely reversed the anti-proliferative activity observed in NALM-6 cells (Fig. 2C).

To determine the magnitude of the apoptotic events, GA-A-treated NALM-6 cells were stained with annexin V which binds to the externalized phosphatidylserine during early stages of apoptosis. Flow cytometric analysis of treated NALM-6 (Fig. 2D, lower left column) showed two separate subpopulations of low forward scatter (FSC) and high side scatter (SSC) profiles characteristic of apoptotic cells. Further analysis of R1 gated cells showed higher proportion of the cells stained with annexin V combining both early and late stage of apoptosis (R2: 23.5% vs. 1.12% in control cells) (Fig. 2D, right column). Apoptotic cells that double-stained with annexin V and PI, suggested further entry of PI into the apoptotic cells at an early stage where damage to the cell membrane occurred. A lower R2 percentage of cell apoptosis was detected in B-cell line 6.16 (6.98 % of equivalent events) (data not shown). Taken together, the above findings suggest that GA-A-induced cell death is mediated by increased caspase expression and activity, which consequently led to apoptotic cell death in B-cell lymphomas.

GA-A TREATMENT REGULATES EXPRESSION OF APOPTOTIC FACTORS

We next examined the molecular mechanisms regulating GA-A-induced apoptosis in lymphoma. Western blot analyses of whole cell lysates were performed for the measurement of anti-apoptotic proteins BCL-2 and survivin, which were then compared with the expression of pro-apoptotic BAX, APAF-1 and cytochrome c following GA-A treatment. Data showed a significant down-regulation of BCL-2 and survivin proteins in GA-A-treated cells, whereas an up-regulation of BAX protein was detected in NALM-6 versus 6.16 cells (Fig. 3A). Analysis of cytoplasmic fractions also showed higher levels of APAF-1 (130 kDa) and cytochrome c proteins in GA-A treated NALM-6 cells (Fig. 3B). Previous studies

suggest that the proapoptotic BH3-only protein BIM plays an important role in BAX-mediated cytochrome c release and induction of apoptosis [Akiyama et al., 2009; Merino et al., 2009; O'Reilly et al., 2000; Zhao et al., 2012]. Thus we examined whether GA-A had any effect on BIM protein expression in B-cell lymphoma. Treatment of lymphoma cells with 20µM GA-A showed that all three isoforms (19, 21 and 24kDa) of BIM were upregulated (Fig. 3A), suggesting that elevated BIM molecules may be involved in BAX activation and possible mitochondrial depolarization.

To determine whether GA-A does indeed induce mitochondrial dysfunction, control and GA-A treated cells were stained with TMRE, washed and analyzed by flow cytometry. Data showed a decreased TMRE fluorescence intensity in GA-A-treated cells compared to vehicle treated cells (Fig. 3C), presumably by depolarizing mitochondrial membrane potential that precedes cytochrome c release into the cytosol. The release of cytochrome c may subsequently promote APAF-1 activation, which in the presence of caspase 9 could form a large multimeric apoptosome [Franklin and Robertson, 2007; Hu et al., 1999], activating the downstream caspase cascades and inducing cell death in lymphoma.

GA-A UPREGULATES HLA CLASS II PRESENTATION AND T CELL RECOGNITION OF LYMPHOMA CELLS

We examined whether GA-A treatment is able to improve antitumor immunity via enhanced HLA class II protein expression in cancer cells, and re-install the functionality of antigen presentation to CD4+ T cells. Western blot analysis of treated cells showed a substantial up-regulation of HLA class II pathway components (HLA-DR, Ii and HLA-DM) in both NALM-6 and 6.16 cells (Supplemental Fig. 1A, B). Flow cytometric analysis confirmed that GA-A treatment slightly, but not significantly increased cell surface HLA-DR4 molecules on NALM-6.DR4 cells when compared with vehicle-treated cells (Supplemental Fig. 1C). A similar pattern of cell surface HLA-DR4 molecules was also observed in GA-A treated 6.16 cells compared to vehicle treated controls (Supplemental Fig. 1C). Next, it was essential to examine if the increased level of class II expression due to GA-A treatment influences lymphoma antigen presentation and re-installs the function of T cell recognition of cancer. Thus, the effects of GA-A treatment on T cell-cancer cell interaction and immune responses were tested in several lymphomas, and were compared with the parallel experiments using professional antigen presenting B-cell lines (6.16 and priess) (Fig. 4). The level of immune recognition was measured by the amount of IL-2 production in the supernatants collected after co-incubation of treated or control cells with the antigen specific CD4+ T cells. Both exogenous (Fig. 4A) and endogenous (Fig. 4B) presentation of antigens by lymphoma cells were significantly enhanced when treated with 10µM or less of GA-A. It was observed that 20µM of GA-A, although anti-proliferative, significantly increased CD4+ T cell recognition of Ramos.DR4, 6.16.DR4.DM and Priess.DR4 cells. Treatment of NALM-6.DR4 and Daudi.DR4 cells with 20µM of GA-A caused relatively lower T cells responses compared to treatment with 10µM of GA-A, presumably due to the greater anti-proliferative effects seen in lymphomas compared to normal B-cells (Fig. 4). Nevertheless, the immune response induced by 20µM GA-A treatment may be biologically significant, since smaller numbers of viable cells were still able to potentiate antigen presentation and immune activation. Taken together, these data suggest that GA-A treatment has the potential to further re-install

antitumor immunity, and it may represent a valuable tool for immune clearance of lymphoma.

GA-A TREATMENT DECREASES TUMOR METASTASIS AND IMPROVES SURVIVAL

To examine the antitumor role of GA-A *in vivo*, we used the well characterized EL4 lymphoma model. In this model, EL4 cells injected into the tail vein of syngeneic C57BL/6 mice metastasize and generate liver tumors [Imai et al., 2007; Knoepp et al., 2008]. Mice bearing EL4 tumor were either left untreated or given a series of intraperitoneal doses of GA-A (60, 50 and 40 mg/kg body weight) at day 10, 14 and 18 respectively. Data showed that mice administered GA-A survived significantly longer than mice treated with vehicle alone (mean survival was 22.25 days vs. 18 days, respectively; n = 8, $p < 0.001$) (Fig. 5A). Untreated or vehicle treated mice showed a slight loss of body weight with an increase in liver size as compared to GA-A treated ones (Fig. 5B). We also detected significantly fewer numbers of liver metastases (tumor nodules) in GA-A-treated mice when compared those with the vehicle-treated mice (Fig. 5C). These data suggest that GA-A is capable of prolonging the survival of EL4 tumor-bearing mice by substantially inhibiting tumor growth and liver metastases.

Serum and spleen/lymph node cells of GA-A-treated and control animals were also tested to determine whether GA-A plays a role in any subsequent *in vivo* immune stimulation. Results showed a slight increase in serum IgG or IgM levels in GA-A-treated mice compared to vehicle-treated controls (Fig. 6A); however, the difference was not statistically significant. Flow cytometric analysis of pooled spleen/lymph node cells showed no significant differences in cell surface expression of MHC-I, MHC-II, or CD86 molecules among GA-A treated and control groups; however, a slight up-regulation of cell surface CD80 expression (MFI: 51.5 vs. 41.2, respectively) was observed (Fig. 6B and data not shown).

MDSCs are believed to be induced by tumor-associated factors, and play an important role in the suppression of host immune responses. Regulatory T cells (Tregs) also play a key role in the maintenance of immunological self-tolerance by suppressing anti-tumor immune responses. While we did not see any significant differences in Tregs (CD4+Foxp3 populations) (Fig. 6C), we detected a profound reduction of MDSCs (CD11b+ Gr-1+ populations) in GA-A-treated mice (Fig. 6D). Further analysis of CD11b+ Gr-1+ populations revealed that GA-A treatment significantly inhibited MDSCs in EL4-beraing mice (Fig. 6E). Histological analysis of liver samples from control and test groups confirmed a marked reduction of metastatic lesions in GA-A treated mice (Fig. 7A). These data suggest that GA-A treatment may have activated cellular immune responses for controlling tumor growth by increased Ag presentation, up-regulation of CD80 molecules and reduction of MDSCs in the host.

One of the key transcription factors involved in the activation of MDSCs is the signal transducer and activator of transcription 3 (STAT3) [Kujawski et al., 2008]. Thus, we tested liver (pooled, n=3) and spleen cells (pooled, n=3) from vehicle and GA-A-treated mice for the status of STAT3 and p-STAT3 by western blotting. As shown in Fig. 7B, GA-A treatment suppressed p-STAT3 levels in spleen cells obtained from GA-A treated mice. To examine if

GA-A treatment influenced cytotoxic CD8+ T cells in the host, we performed both surface and intracellular flow cytometric analysis for determining IFN-γ producing CD8+ T cells in the spleen cells. Data obtained from this assay showed that GA-A treatment markedly increased the number of IFN-γ producing CD8+ T cells as compared to vehicle controls (Fig. 7C), suggesting that GA-A has a potential to induce antitumor immunity, and to reduce the burden of metastatic lymphoma.

DISCUSSION

Currently used chemotherapy regimens for lymphoid malignancies, although effective in many cases, have the drawback of exhibiting high levels of treatment-associated toxicities; these effects are even more pronounced in elderly patients [Campbell et al., 2012; Yamaguchi et al., 2011; Zhou et al., 2012]. Another drawback to traditional chemotherapies is the resistance of a small percentage of tumors to treatment, resulting in long-term therapy and eventually disease relapse [Borchmann et al., 2012; Hann and Keseru, 2012]. Thus, the search for new natural antitumor compounds with significant anti-growth activity and the ability to restore immunogenicity of target cancer cells has increasingly become a focus in the development of novel treatment strategies for lymphoma. The ability to generate an immune response against chemotherapy-resistant tumor cells could ultimately restore immunity and lead to further tumor clearance. The present study shows clearly that *G. lucidum*-derived triterpenoid GA-A exhibits profound antitumor properties through inhibition of cell proliferation, alteration of intracellular signaling pathways, and induction of apoptosis. Treatment with GA-A induced a remarkable dose-dependent anti-proliferative activity in lymphoma cell lines as well as primary tumors, with a significantly lower anti-growth activity to healthy cells. In addition to its anti-proliferative effects on tumor cells, our data highlights for the first time that GA-A is capable of enhancing HLA class II-mediated antigen presentation and CD4+ T cell recognition of B-cell lymphomas. GA-A treatment up-regulated both intracellular and surface expression of HLA class II molecules in B-cell lymphomas, which correlated with enhanced antigen presentation and CD4+ T cell stimulation. Although GA-A has a greater anti-growth activity in lymphoma cells compared to antigen presenting B-lymphoblastoid cells, the relatively fewer viable lymphoma cells were still capable of stimulating a strong T cell response *in vitro*.

Apoptosis, a mechanism of programmed cell death, is thought to be a key mechanism to maintaining tissue homeostasis, especially in the hematopoietic system [Fecteau and Kipps, 2012; Kerr et al., 1994; Kerr et al., 1972]. Thus, resistance to apoptotic cell death can contribute to the development of hematological malignancies. Our data suggest that GA-A induces caspase-dependent apoptosis as a major pathway for inducing cell death. The mechanism of cell death was supported by up-regulation and cleavage of caspases 3, 8, and 9. Caspase expression correlated with an increase in catalytic activity of cellular caspases. Furthermore, when cellular caspases were inhibited by Z-VAD-FMK, anti-proliferative activity was drastically reduced, suggesting a key role for effector caspases in executing GA-A-induced cell death. Our results imply that the apoptotic events were regulated, at least in part, by up-regulation of the pro-apoptotic BH3-only protein BIM and multi-BH domain pro-apoptotic protein BAX and down-regulation of the anti-apoptotic protein BCL-2. Analysis of cytoplasmic fractions of GA-A-treated cells showed a significant up-regulation

of APAF-1 accompanied with a greater release of mitochondrial cytochrome c in lymphoma cells compared to healthy B-cell counterpart. These findings suggest a possible scenario of inducing the intrinsic apoptotic pathway initiated by the migration of BAX to the surface of the mitochondria where it subsequently inhibits the antiapoptotic effects of BCL-2. We suggest that GA-A induced reduction of BCL-2/BAX ratio caused dysfunction in mitochondrial membrane potential, which was indicated by a lower TMRE staining of treated cells causing cytochrome c release. The release of cytochrome c is crucial because it can promote APAF-1 activation, facilitating the formation of a large multimeric apoptosome that activates downstream effector caspases leading to an induction of apoptosis in lymphoma cells.

In order to investigate the potential therapeutic relevance of our *in vitro* data, the antitumor effects of GA-A were examined *in vivo* using a syngeneic EL4 lymphoma mouse model. We found that administration of GA-A significantly suppressed metastasis of EL4 lymphoma cells to the liver, which correlated with improved survival. While Tregs are often associated with a poor clinical outcome [Facciabene et al., 2012], this study didn't find any significant changes in Treg cells in vehicle vs GA-A treated mice. By contrast, we have found GA-A treatment attenuates EL4 tumor growth and metastasis by a marked inhibition of MDSC populations in the host, which could be regulated via the STAT3 pathway [Kujawski et al., 2008]. It is now well recognized that MDSCs promote immune escape of tumor cells via inhibition of T cell responses, resulting tumor growth and metastasis [Deng et al., 2014; Sawant et al., 2013; Wesolowski et al., 2013]. Interesting, the reduction of MDSCs correlated with increased number of IFN-γ producing CD8+ T cells, which might have played a critical role in reducing tumor burden in GA-A treated animals. Constitutive activation of STAT3 in MDSCs also up-regulates anti-apoptotic, pro-proliferative, and pro-angiogenic factors; thus, inhibition of STAT3 phosphorylation by GA-A treatment could have accomplished the therapeutic outcome in this model. Recent studies have also supported the involvement of MDSCs as a prognostic factor in various clinical settings and the possible therapeutic approaches towards elimination of their immunosuppressive activity and enhancement of antitumor immune responses [Deng et al., 2014; Srivastava et al., 2012a; Wesolowski et al., 2013]. It is also important to note that MDSCs are well studied in various tumor-bearing hosts where they are significantly expanded and suppress anti-tumor immune responses compared to naive counterparts [Poschke et al., 2012; Srivastava et al., 2012b]. In conclusion, this study suggests that GA-A possesses several antitumor properties that make it an attractive candidate for the development of novel therapeutics. First, it exhibits significant and selective anti-growth activity towards cancer cells. This may provide a targeted mechanism whereby tumor cells can be cleared with limited side effects. Secondly, at lower doses, GA-A induces up-regulation of HLA class II that may prove to enhanced Ag presentation and T cell recognition of target cancer cells. Third, GA-A attenuates MDSC populations possibly by inhibiting phosphorylation of STAT3. Fourth, GA-A treatment potentiates antitumor immune responses by activating IFN-γ producing CD8+ T cells. Finally, the amelioratory effects of GA-A were shown *in vivo* as evidenced by the increased survival rate that correlated with a significant decrease in tumor metastasis among treated animals.

Supplementary Material

Refer to Web version on PubMed Central for supplementary material.

Acknowledgments

References

Akiyama T, Dass CR, Choong PF. Bim-targeted cancer therapy: a link between drug action and underlying molecular changes. Mol Cancer Ther. 2009; 8:3173–80. [PubMed: 19934277]

Amria S, Cameron C, Stuart R, Haque A. Defects in HLA class II antigen presentation in B-cell lymphomas. Leuk Lymphoma. 2008; 49:353–5. [PubMed: 18231926]

Boh B, Berovic M, Zhang J, Zhi-Bin L. Ganoderma lucidum and its pharmaceutically active compounds. Biotechnol Annu Rev. 2007; 13:265–301. [PubMed: 17875480]

Borchmann P, Eichenauer DA, Engert A. State of the art in the treatment of Hodgkin lymphoma. Nat Rev Clin Oncol. 2012; 9:450–9. [PubMed: 22688578]

Campbell BA, Connors JM, Gascoyne RD, Morris WJ, Pickles T, Sehn LH. Limited-stage diffuse large B-cell lymphoma treated with abbreviated systemic therapy and consolidation radiotherapy: involved-field versus involved-node radiotherapy. Cancer. 2012; 118:4156–65. [PubMed: 22252721]

Chen HS, Tsai YF, Lin S, Lin CC, Khoo KH, Lin CH, Wong CH. Studies on the immuno-modulating and anti-tumor activities of Ganoderma lucidum (Reishi) polysaccharides. Bioorg Med Chem. 2004; 12:5595–601. [PubMed: 15465337]

Deng L, Liang H, Burnette B, Beckett M, Darga T, Weichselbaum RR, Fu YX. Irradiation and anti-PD-L1 treatment synergistically promote antitumor immunity in mice. J Clin Invest. 2014; 124:687–95. [PubMed: 24382348]

Drenou B, Tilanus M, Semana G, Alizadeh M, Birebent B, Grosset JM, Dias P, van Wichen D, Arts Y, De Santis D, Fauchet R, Amiot L. Loss of heterozygosity, a frequent but a non-exclusive mechanism responsible for HLA dysregulation in non-Hodgkin's lymphomas. Br J Haematol. 2004; 127:40–9. [PubMed: 15384976]

Facciabene A, Motz GT, Coukos G. T-regulatory cells: key players in tumor immune escape and angiogenesis. Cancer Res. 2012; 72:2162–71. [PubMed: 22549946]

Fecteau JF, Kipps TJ. Structure and function of the hematopoietic cancer niche: focus on chronic lymphocytic leukemia. Front Biosci (Schol Ed). 2012; 4:61–73. [PubMed: 22202043]

Franklin EE, Robertson JD. Requirement of Apaf-1 for mitochondrial events and the cleavage or activation of all procaspases during genotoxic stress-induced apoptosis. Biochem J. 2007; 405:115–22. [PubMed: 17348858]

God JM, Zhao D, Cameron CA, Amria S, Bethard JR, Haque A. Disruption of HLA class II antigen presentation in Burkitt lymphoma: implication of a 47,000 MW acid labile protein in CD4+ T-cell recognition. Immunology. 2014; 142:492–505. [PubMed: 24628049]

Goh C, Narayanan S, Hahn YS. Myeloid-derived suppressor cells: the dark knight or the joker in viral infections? Immunol Rev. 2013; 255:210–21. [PubMed: 23947357]

Goldstein OG, Hajiaghamohseni LM, Amria S, Sundaram K, Reddy SV, Haque A. Gamma-IFN-inducible-lysosomal thiol reductase modulates acidic proteases and HLA class II antigen processing in melanoma. Cancer Immunol Immunother. 2008; 57:1461–70. [PubMed: 18343923]

Hann MM, Keseru GM. Finding the sweet spot: the role of nature and nurture in medicinal chemistry. Nat Rev Drug Discov. 2012; 11:355–65. [PubMed: 22543468]

Haque A, Hajiaghamohseni LM, Li P, Toomy K, Blum JS. Invariant chain modulates HLA class II protein recycling and peptide presentation in nonprofessional antigen presenting cells. Cell Immunol. 2007; 249:20–9. [PubMed: 18067883]

Haque MA, Hawes JW, Blum JS. Cysteinylation of MHC class II ligands: peptide endocytosis and reduction within APC influences T cell recognition. J Immunol. 2001; 166:4543–51. [PubMed: 11254711]

Haque MA, Li P, Jackson SK, Zarour HM, Hawes JW, Phan UT, Maric M, Cresswell P, Blum JS. Absence of gamma-interferon-inducible lysosomal thiol reductase in melanomas disrupts T cell recognition of select immunodominant epitopes. J Exp Med. 2002; 195:1267–77. [PubMed: 12021307]

Hiraiwa A, Yamanaka K, Kwok WW, Mickelson EM, Masewicz S, Hansen JA, Radka SF, Nepom GT. Structural requirements for recognition of the HLA-Dw14 class II epitope: a key HLA determinant associated with rheumatoid arthritis. Proc Natl Acad Sci U S A. 1990; 87:8051–5. [PubMed: 1700425]

Hossain A, God JM, Radwan FF, Amria S, Zhao D, Bethard JR, Haque A. HLA class II defects in Burkitt lymphoma: bryostatin-1-induced 17 kDa protein restores CD4+ T-cell recognition. Clin Dev Immunol. 2011; 2011:780839. [PubMed: 22162713]

Hossain A, Radwan FF, Doonan BP, God JM, Zhang L, Bell PD, Haque A. A possible cross-talk between autophagy and apoptosis in generating an immune response in melanoma. Apoptosis. 2012; 17:1066–78. [PubMed: 22847295]

Hsieh TC, Wu JM. Suppression of proliferation and oxidative stress by extracts of Ganoderma lucidum in the ovarian cancer cell line OVCAR-3. Int J Mol Med. 2011; 28:1065–9. [PubMed: 21887458]

Hu Y, Benedict MA, Ding L, Nunez G. Role of cytochrome c and dATP/ATP hydrolysis in Apaf-1-mediated caspase-9 activation and apoptosis. EMBO J. 1999; 18:3586–95. [PubMed: 10393175]

Imai M, Ohta R, Varela JC, Song H, Tomlinson S. Enhancement of antibody-dependent mechanisms of tumor cell lysis by a targeted activator of complement. Cancer Res. 2007; 67:9535–41. [PubMed: 17909064]

Jiang J, Grieb B, Thyagarajan A, Sliva D. Ganoderic acids suppress growth and invasive behavior of breast cancer cells by modulating AP-1 and NF-kappaB signaling. Int J Mol Med. 2008; 21:577–84. [PubMed: 18425349]

Kennedy BC, Shimato S, Anderson RC, Bruce JN. Defining the mechanisms of CD8 T-cell tumor tolerance. Immunotherapy. 2011; 3:23–6. [PubMed: 21174554]

Kerr JF, Winterford CM, Harmon BV. Apoptosis. Its significance in cancer and cancer therapy. Cancer. 1994; 73:2013–26. [PubMed: 8156506]

Kerr JF, Wyllie AH, Currie AR. Apoptosis: a basic biological phenomenon with wide-ranging implications in tissue kinetics. Br J Cancer. 1972; 26:239–57. [PubMed: 4561027]

Khaled YS, Ammori BJ, Elkord E. Myeloid-derived suppressor cells in cancer: recent progress and prospects. Immunol Cell Biol. 2013; 91:493–502. [PubMed: 23797066]

Kimura Y, Taniguchi M, Baba K. Antitumor and antimetastatic effects on liver of triterpenoid fractions of Ganoderma lucidum: mechanism of action and isolation of an active substance. Anticancer Res. 2002; 22:3309–18. [PubMed: 12530080]

Knoepp SM, Chahal MS, Xie Y, Zhang Z, Brauner DJ, Hallman MA, Robinson SA, Han S, Imai M, Tomlinson S, Meier KE. Effects of active and inactive phospholipase D2 on signal transduction, adhesion, migration, invasion, and metastasis in EL4 lymphoma cells. Mol Pharmacol. 2008; 74:574–84. [PubMed: 18523140]

Kovats S, Nepom GT, Coleman M, Nepom B, Kwok WW, Blum JS. Deficient antigen-presenting cell function in multiple genetic complementation groups of type II bare lymphocyte syndrome. J Clin Invest. 1995; 96:217–23. [PubMed: 7615790]

Kujawski M, Kortylewski M, Lee H, Herrmann A, Kay H, Yu H. Stat3 mediates myeloid cell-dependent tumor angiogenesis in mice. J Clin Invest. 2008; 118:3367–77. [PubMed: 18776941]

Li F, Wang Y, Wang X, Li J, Cui H, Niu M. Ganoderic acids suppress growth and angiogenesis by modulating the NF-kappaB signaling pathway in breast cancer cells. Int J Clin Pharmacol Ther. 2012; 50:712–21. [PubMed: 22762853]

Liu RM, Li YB, Zhong JJ. Cytotoxic and pro-apoptotic effects of novel ganoderic acid derivatives on human cervical cancer cells in vitro. Eur J Pharmacol. 2012; 681:23–33. [PubMed: 22366428]

Merino D, Giam M, Hughes PD, Siggs OM, Heger K, O'Reilly LA, Adams JM, Strasser A, Lee EF, Fairlie WD, Bouillet P. The role of BH3-only protein Bim extends beyond inhibiting Bcl-2-like prosurvival proteins. J Cell Biol. 2009; 186:355–62. [PubMed: 19651893]

Morkowski S, Goldrath AW, Eastman S, Ramachandra L, Freed DC, Whiteley P, Rudensky A. T cell recognition of major histocompatibility complex class II complexes with invariant chain processing intermediates. J Exp Med. 1995; 182:1403–13. [PubMed: 7595211]

Mougiakakos D, Jitschin R, von Bahr L, Poschke I, Gary R, Sundberg B, Gerbitz A, Ljungman P, Le Blanc K. Immunosuppressive CD14+HLA-DRlow/neg IDO+ myeloid cells in patients following allogeneic hematopoietic stem cell transplantation. Leukemia. 2013; 27:377–88. [PubMed: 22828446]

O'Reilly LA, Cullen L, Visvader J, Lindeman GJ, Print C, Bath ML, Huang DC, Strasser A. The proapoptotic BH3-only protein bim is expressed in hematopoietic, epithelial, neuronal, and germ cells. Am J Pathol. 2000; 157:449–61. [PubMed: 10934149]

Ocker M, Hopfner M. Apoptosis-modulating drugs for improved cancer therapy. Eur Surg Res. 2012; 48:111–20. [PubMed: 22538523]

Poschke I, Mao Y, Adamson L, Salazar-Onfray F, Masucci G, Kiessling R. Myeloid-derived suppressor cells impair the quality of dendritic cell vaccines. Cancer Immunol Immunother. 2012; 61:827–38. [PubMed: 22080405]

Radwan FF, Zhang L, Hossain A, Doonan BP, God JM, Haque A. Mechanisms regulating enhanced human leukocyte antigen class II-mediated CD4 + T cell recognition of human B-cell lymphoma by resveratrol. Leuk Lymphoma. 2012; 53:305–14. [PubMed: 21854084]

Sadava D, Still DW, Mudry RR, Kane SE. Effect of Ganoderma on drug-sensitive and multidrug-resistant small-cell lung carcinoma cells. Cancer Lett. 2009; 277:182–9. [PubMed: 19188016]

Sawant A, Schafer CC, Jin TH, Zmijewski J, Tse HM, Roth J, Sun Z, Siegal GP, Thannickal VJ, Grant SC, Ponnazhagan S, Deshane JS. Enhancement of antitumor immunity in lung cancer by targeting myeloid-derived suppressor cell pathways. Cancer Res. 2013; 73:6609–20. [PubMed: 24085788]

Siegel R, DeSantis C, Virgo K, Stein K, Mariotto A, Smith T, Cooper D, Gansler T, Lerro C, Fedewa S, Lin C, Leach C, Cannady RS, Cho H, Scoppa S, Hachey M, Kirch R, Jemal A, Ward E. Cancer treatment and survivorship statistics, 2012. CA Cancer J Clin. 2012; 62:220–41. [PubMed: 22700443]

Sliva D. Ganoderma lucidum (Reishi) in cancer treatment. Integr Cancer Ther. 2003; 2:358–64. [PubMed: 14713328]

Souza AC, de Fatima A, da Silveira RB, Justo GZ. Seek and destroy: the use of natural compounds for targeting the molecular roots of cancer. Curr Drug Targets. 2012; 13:1072–82. [PubMed: 22594475]

Srivastava MK, Zhu L, Harris-White M, Huang M, St John M, Lee JM, Salgia R, Cameron RB, Strieter R, Dubinett S, Sharma S. Targeting myeloid-derived suppressor cells augments antitumor activity against lung cancer. Immunotargets Ther. 2012a; 2012:7–12. [PubMed: 24791250]

Srivastava MK, Zhu L, Harris-White M, Kar U, Huang M, Johnson MF, Lee JM, Elashoff D, Strieter R, Dubinett S, Sharma S. Myeloid suppressor cell depletion augments antitumor activity in lung cancer. PLoS One. 2012b; 7:e40677. [PubMed: 22815789]

Surjit M, Kumar R, Mishra RN, Reddy MK, Chow VT, Lal SK. The severe acute respiratory syndrome coronavirus nucleocapsid protein is phosphorylated and localizes in the cytoplasm by 14-3-3-mediated translocation. J Virol. 2005; 79:11476–86. [PubMed: 16103198]

Wesolowski R, Markowitz J, Carson WE 3rd. Myeloid derived suppressor cells – a new therapeutic target in the treatment of cancer. J Immunother Cancer. 2013; 1:10. [PubMed: 24829747]

Wu GS, Lu JJ, Guo JJ, Li YB, Tan W, Dang YY, Zhong ZF, Xu ZT, Chen XP, Wang YT. Ganoderic acid DM, a natural triterpenoid, induces DNA damage, G1 cell cycle arrest and apoptosis in human breast cancer cells. Fitoterapia. 2012; 83:408–14. [PubMed: 22178684]

Wubshet SG, Johansen KT, Nyberg NT, Jaroszewski JW. Direct (13)C NMR detection in HPLC hyphenation mode: analysis of Ganoderma lucidum terpenoids. J Nat Prod. 2012; 75:876–82. [PubMed: 22515483]

Yamaguchi H, Hirakawa T, Inokuchi K. Importance of relative dose intensity in chemotherapy for diffuse large B-cell lymphoma. J Clin Exp Hematop. 2011; 51:1–5. [PubMed: 21628854]

Yao X, Li G, Xu H, Lu C. Inhibition of the JAK-STAT3 signaling pathway by ganoderic acid A enhances chemosensitivity of HepG2 cells to cisplatin. Planta Med. 2012; 78:1740–8. [PubMed: 22961117]

Younger AR, Amria S, Jeffrey WA, Mahdy AE, Goldstein OG, Norris JS, Haque A. HLA class II antigen presentation by prostate cancer cells. Prostate Cancer Prostatic Dis. 2008; 11:334–41. [PubMed: 17938645]

Zhao D, Amria S, Hossain A, Sundaram K, Komlosi P, Nagarkatti M, Haque A. Enhancement of HLA class II-restricted CD4+ T cell recognition of human melanoma cells following treatment with bryostatin-1. Cell Immunol. 2011; 271:392–400. [PubMed: 21903207]

Zhao L, He F, Liu H, Zhu Y, Tian W, Gao P, He H, Yue W, Lei X, Ni B, Wang X, Jin H, Hao X, Lin J, Chen Q. Natural diterpenoid compound elevates expression of Bim protein, which interacts with antiapoptotic protein Bcl-2, converting it to proapoptotic Bax-like molecule. J Biol Chem. 2012; 287:1054–65. [PubMed: 22065578]

Zhou Y, You MJ, Young KH, Lin P, Lu G, Medeiros LJ, Bueso-Ramos CE. Advances in the molecular pathobiology of B-lymphoblastic leukemia. Hum Pathol. 2012; 43:1347–62. [PubMed: 22575265]
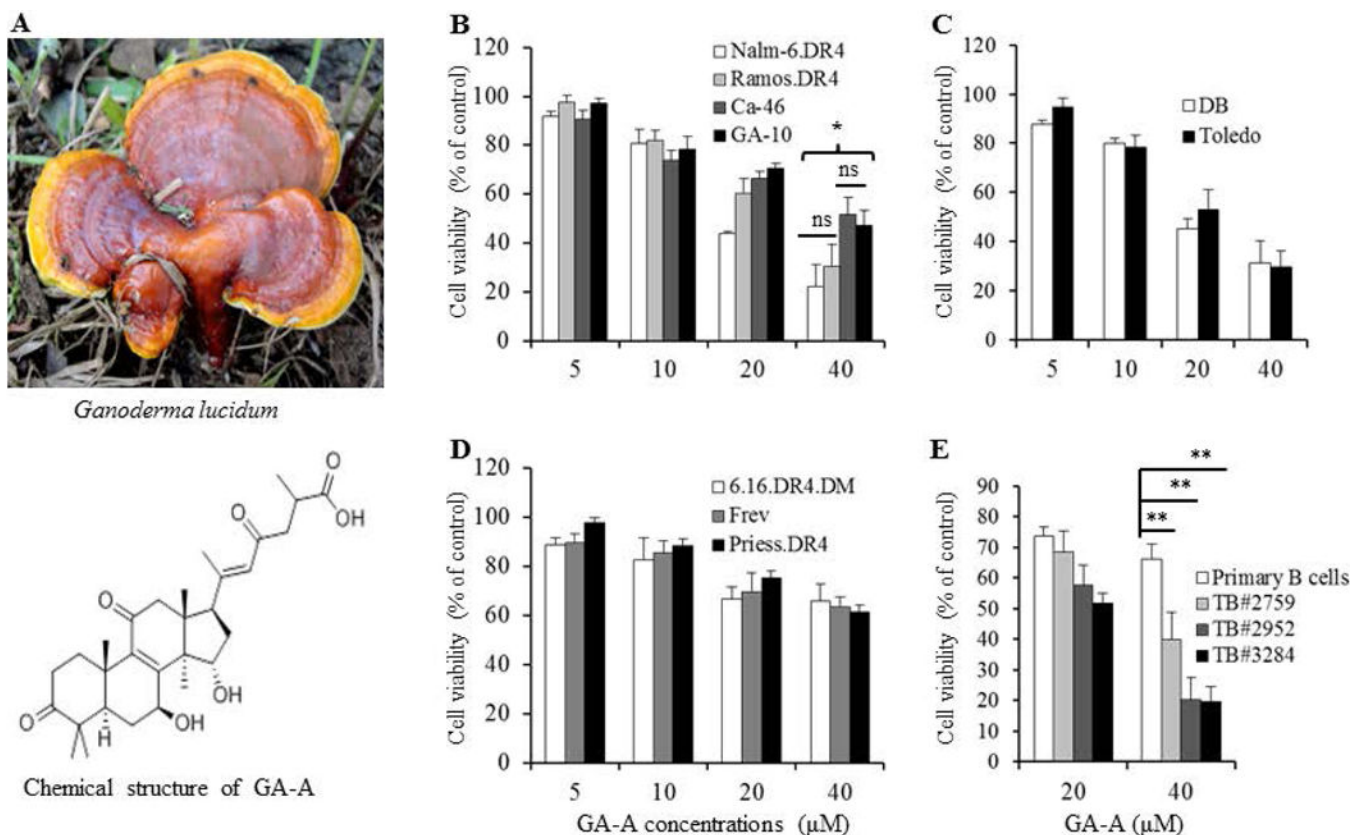
Fig. 1.
The chemical structure of the triterpenoid [Ganoderic acid A (GA-A)], and GA-A's anti-proliferative activity in B-lymphoma cells. (A) GA-A chemical structure. (B) A pre-B acute lymphocytic leukemia line (NALM-6), Burkitt's lymphoma (Ramos, CA-46 and GA-10), (C) non-Hodgkin's lymphoma (DB and Toledo), (D) B-lymphoblastoid cell lines (6.16.DR4.DM, Frev and Priess), and (E) primary B-cells from lymphoma patients and healthy individuals were treated with GA-A (5–40μM) for 24h, followed by a cell viability assay as described in the methods section. Control cells treated with vehicle alone were utilized to calculate the percent anti-proliferative activity induced by GA-A as indicated. Primary B-cells obtained from lymphoma patients include follicular B-cell lymphoma (TB#2759), diffuse large B-cell lymphoma (TB#2952), and chronic lymphocytic leukemia (TB#3284). These cells were treated with vehicle alone or GA-A, and viable cells were counted using trypan blue dye exclusion. The percent cell viability as compared to control was calculated as described in the methods. The data shown are results of at least three separate experiments performed in triplicate wells. Error bars represent mean ± S.D. Significant differences were indicated as (*$p<0.05$, **$p<0.01$), where ns indicates (not significant).
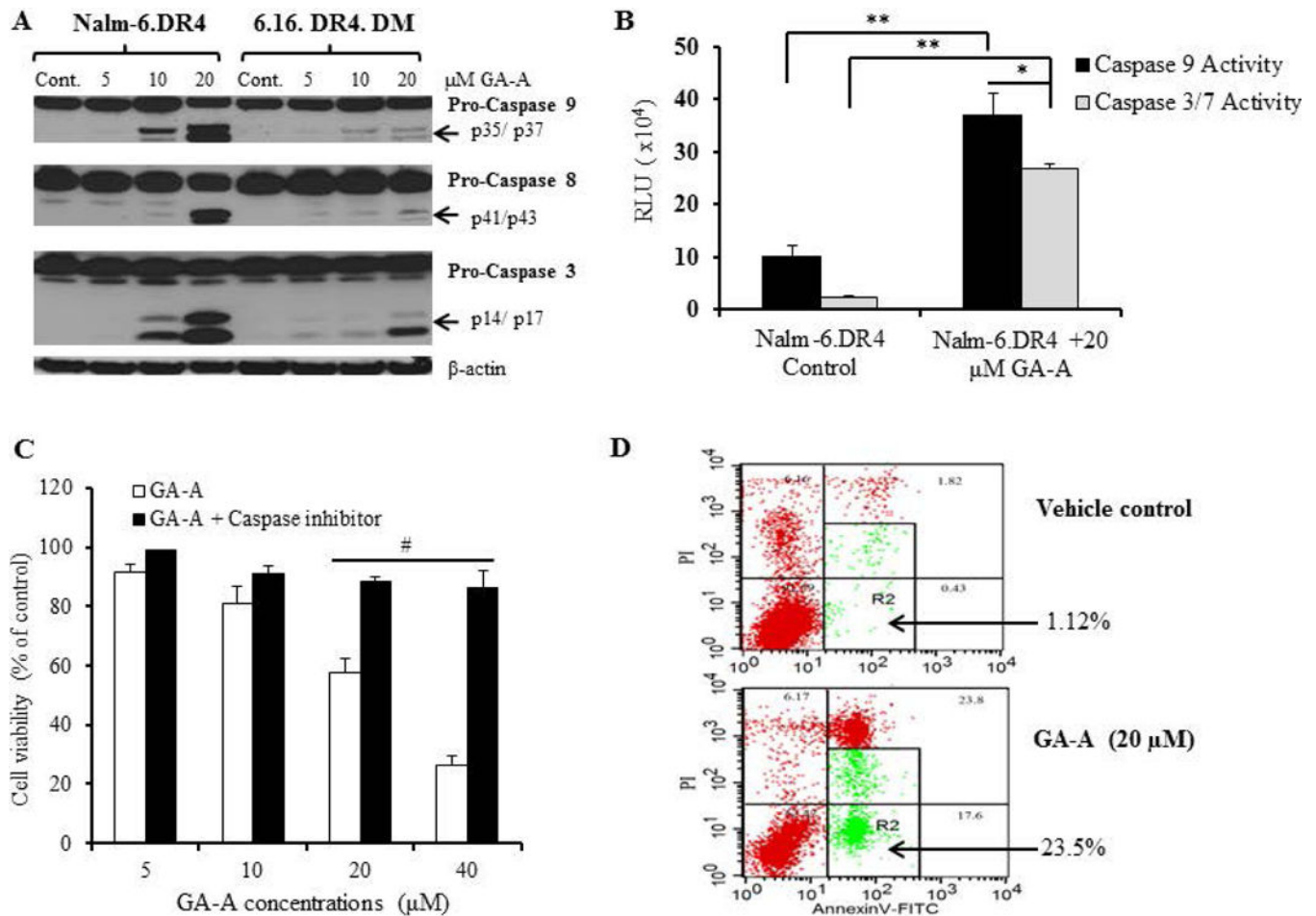
Fig. 2.

GA-A induces caspase-dependent apoptosis in B-cell lymphoma. (A) Western blot analysis showing protein expression and cleavage of active caspases 9, 8, and 3 in cells treated with GA-A (5–20μM) or vehicle alone (control) as described in the methods. β-actin was utilized as a loading control. (B) Caspase activity was measured in cells treated with GA-A (20μM) or vehicle alone for 24h at 37°C in 96-well plate as described. The plate was equilibrated to 22°C, followed by the addition of Caspase-Glo® 9 or Caspase-Glo® 3/7 reagents as per manufacturer recommendations. Luminescence was recorded at 30 min after adding the reagent. (C) Inhibition of caspases by a pan caspase inhibitor (Z-VAD-FMK) blocked GA-A-induced anti-proliferative activity in NALM-6.DR4 pre-B acute lymphocytic leukemia cells. Cells were treated with GA-A (5, 10, 20 and 40μM) or vehicle alone and incubated with or without Z-VAD-FMK for 24h at 37°C, followed by the MTS viability assay and calculation of anti-proliferative responses as described in the methods. The data shown are representative of at least three separate experiments. Error bars represent mean ± S.D. (D) Contour diagrams of annexin V-FITC/PI flow cytometry of NALM-6.DR4 cells after 20μM of GA-A treatment for 24h. Dot plot of forward and side scatter (20,000 events/sample, left panels), and annexin V/PI double staining (right panels) were shown. The R2 quadrants represent the annexin V-positive early and late apoptotic cells. The figures shown are representatives of at least three independent experiments with similar patterns, and error bars
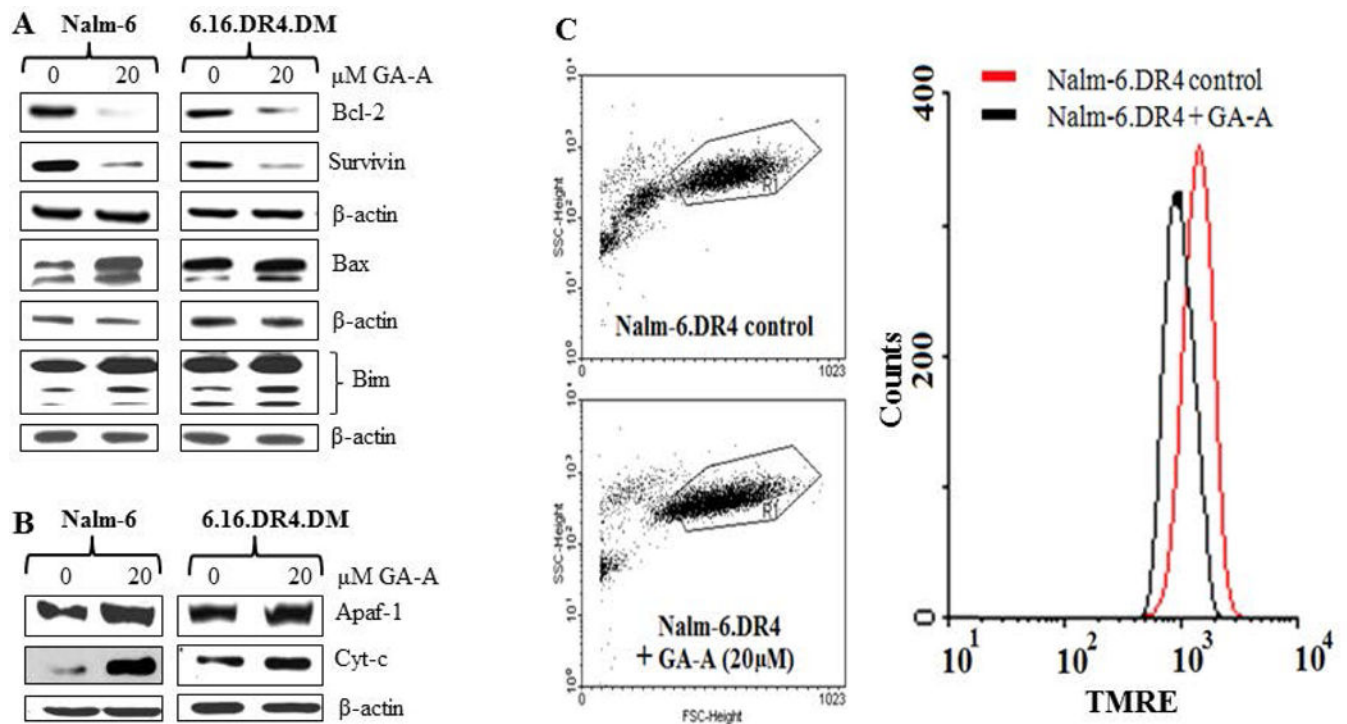
represent average ± S.D. Significant differences were calculated by student's *t* test; *p<0.05, **p<0.01, [#]p<0.001.

Fig. 3.
GA-A treatment alters apoptosis regulatory molecules in B-lymphoma cells. (A) Western blot analysis of whole cell lysates showing suppression of anti-apoptotic molecules BCL-2 and survivin, and an up-regulation of pro-apoptotic BIM, BAX proteins in NALM-6.DR4 and 6.16.DR4.DM cells treated with GA-A (0 and 20μM) for 24 h. (B) Western blot analysis showing an up-regulation of APAF-1 and cytochrome c proteins in enriched cytoplasmic fractions of NALM-6.DR4 and 6.16.DR4.DM cells. Cells were treated with vehicle alone or GA-A for 24h, and were subjected to Western blotting for BCL-2, Survivin, BAX, BIM, APAF-1 and cytochrome c proteins. β-actin was used as a loading control. (C) Flow cytometry analysis of TMRE stained NALM-6.DR4 cells after 20μM of GA-A treatment for 24h at 37°C. Left panels show dot plots of forward and side scatter (20,000 events/sample) obtained from control and GA-A-treated cells. Right panel shows histograms extracted from dot plots of TMRE staining of control (red line) and GA-A treated (black line) cells. Data are representative of at least three independent experiments.
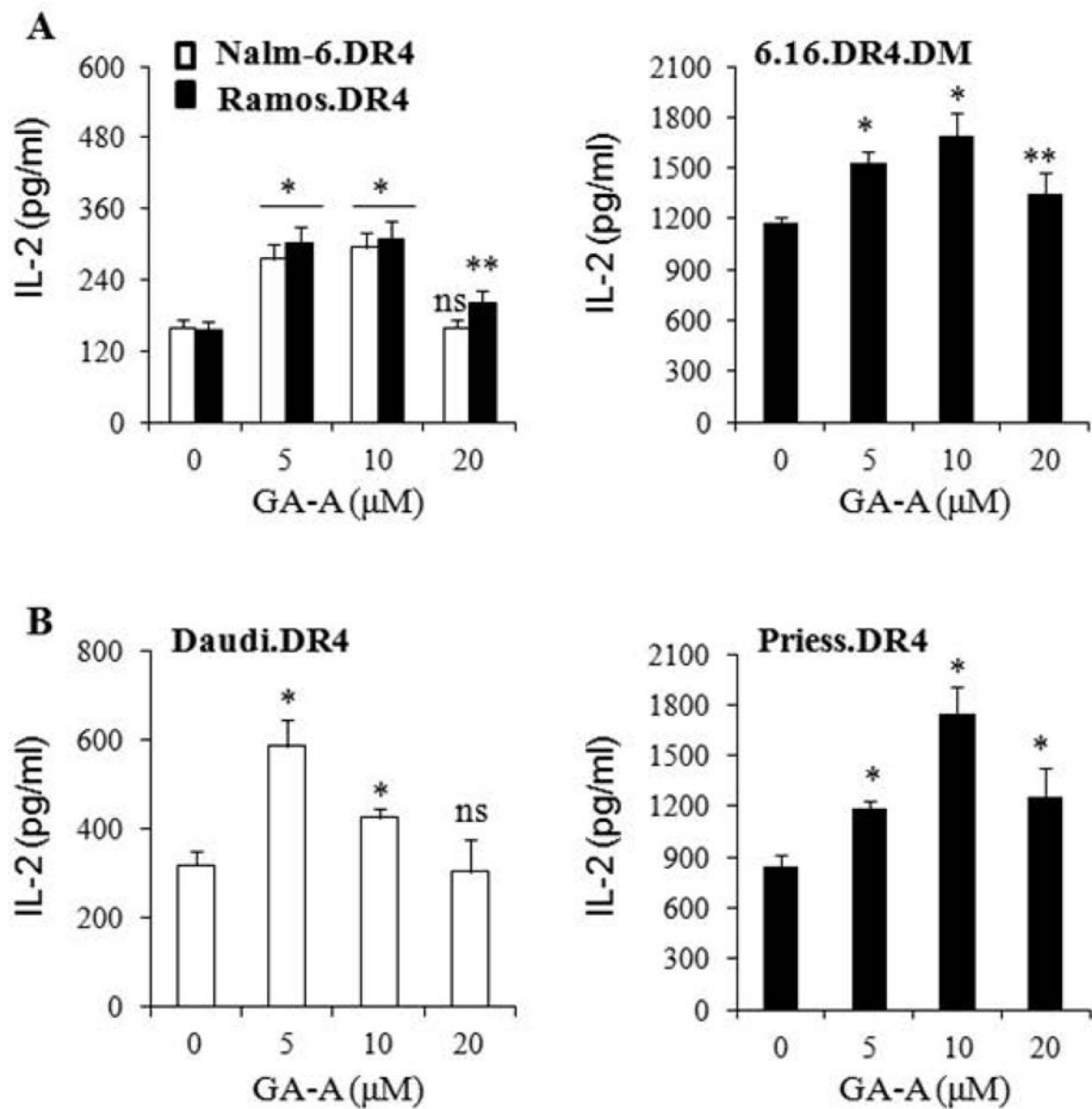
Fig. 4.
GA-A treatment enhances antigen presentation by B-cell lymphoma cells to CD4+ T cells. (A) Exogenous Ag presentation and immune recognition of NALM-6.DR4, Ramos.DR4 and 6.16 DR4.DM cells. Cells were first seeded in 96-well plates and treated with GA-A (5–20μM) or vehicle alone for 24 h. Following treatment, cells were incubated with HSA_{64-76K} peptide for another 4h, washed and co-cultured with the HSA_{64-76K} peptide specific T cell hybridoma for 24h. (B) Endogenous Ag presentation and CD4+ T cell recognition of Daudi.DR4 and Priess cells. Daudi.DR4 and Priess.DR4 cell lines, which express endogenous IgGκ were cocultured with the $IgG\kappa_{188-203}$ peptide specific T cells in the absence of exogenously added Ags/peptides. The extent of antigen presentation is featured by the increase in IL-2 production due to T cell proliferation. IL-2 was measured by ELISA and expressed as pg/ml ± SD of triplicate wells of at least three independent experiments.

Effects of GA-A on Ag presentation were calculated as compared to untreated controls. *p<0.01, **p<0.05, ns = not significant.
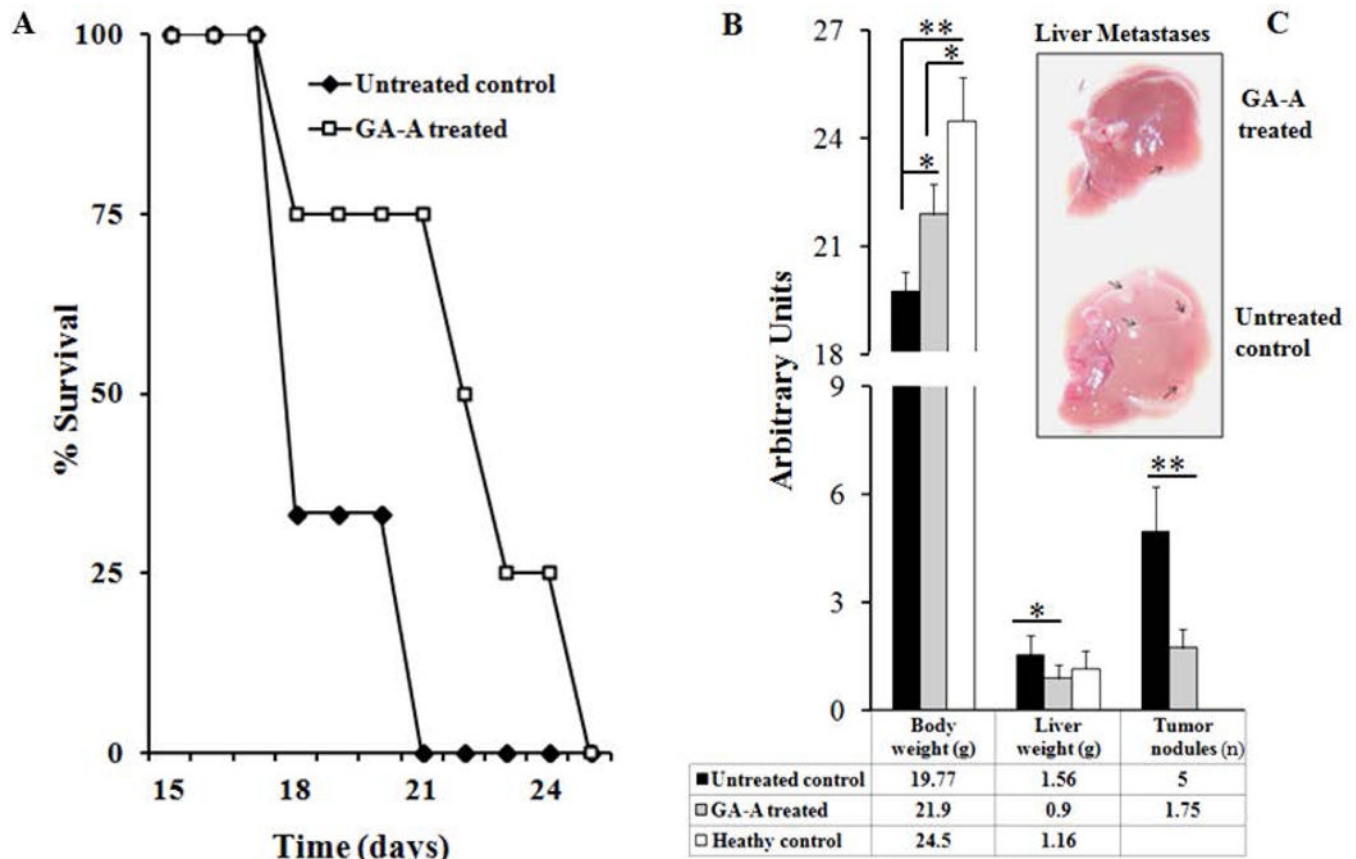
Fig. 5.
GA-A treatment reduces metastatic growth of lymphoma *in vivo*. Syngeneic male mice were injected with EL4 cell line as described in Materials and Methods. (A) Figure showing survival study of GA-A treated and untreated control mice. Eight mice were used in each treatment group. Results are expressed as a percentage of the initial group surviving at each time point (average survival for GA-A treated and untreated control was 22.25 days vs. 18 days, respectively; n = 8, p = 0.0003). (B) Average weights of whole body and liver, as well as the average number of tumor nodules were counted on the surface of liver samples and expressed as arbitrary units. Quantitative data were shown in the table below. (C) A representative photograph of liver samples collected from GA-A and vehicle treated animals, showing the abundance of tumor nodules in untreated controls (arrows). Significant differences were calculated by student's *t*-test; **p<0.01.
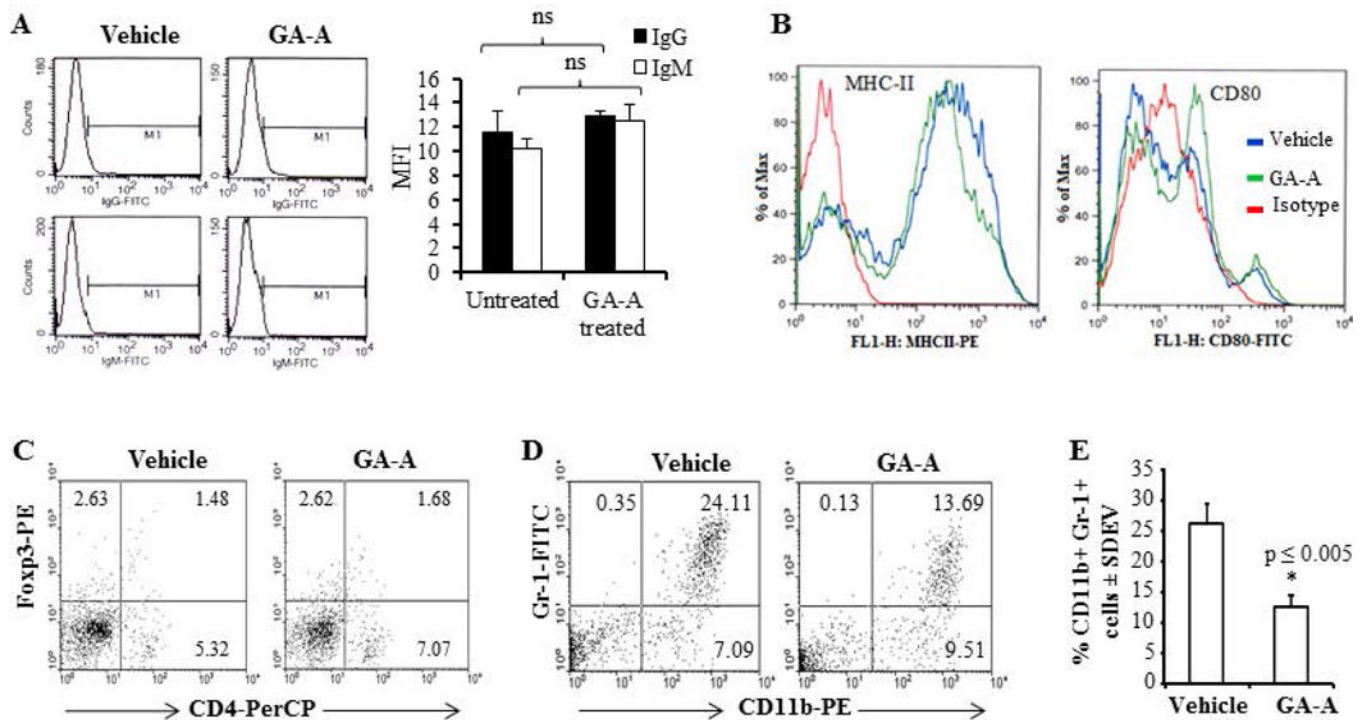
Fig. 6.
GA-A treatment reduces myeloid-derived suppressor cells in EL4 mouse lymphoma model. (A) Representative MFI data obtained from flow cytometric analyses of IgG and IgM in the sera collected from of GA-A treated and control mice as described in the methods section. Significant differences were calculated by student's *t* test. ns = not significant. (B) Flow cytometric analysis of cell surface expression of MHC class II and CD80 molecules in pooled lymph node/spleen cells collected from GA-A-treated and vehicle-treated mice as described. (C-D) Flow cytometric analysis of Tregs (CD4+ Foxp3) and MDSC (Gr-1+ CD11b) populations following GA-A treatment. Mice were first injected with EL4 cells and treated with vehicle alone (50μl of DMSO) or GA-A (50mg/kg body weight, 1mg/50μl of DMSO) three times (days 10, 14 and 18). On day 20, lymph node/spleens were harvested and single cell suspensions were made, pooled and processed for intracellular staining. Flow cytometric analysis was performed for detecting Tregs and MDSC populations in control and GA-A treated mice as described in the methods. (E) A representative histogram showing %CD11b+Gr-1+ cells in vehicle vs. GA-A-treated pooled spleen cells. Data are representative of three independent experiments with similar patterns. ns = not significant.
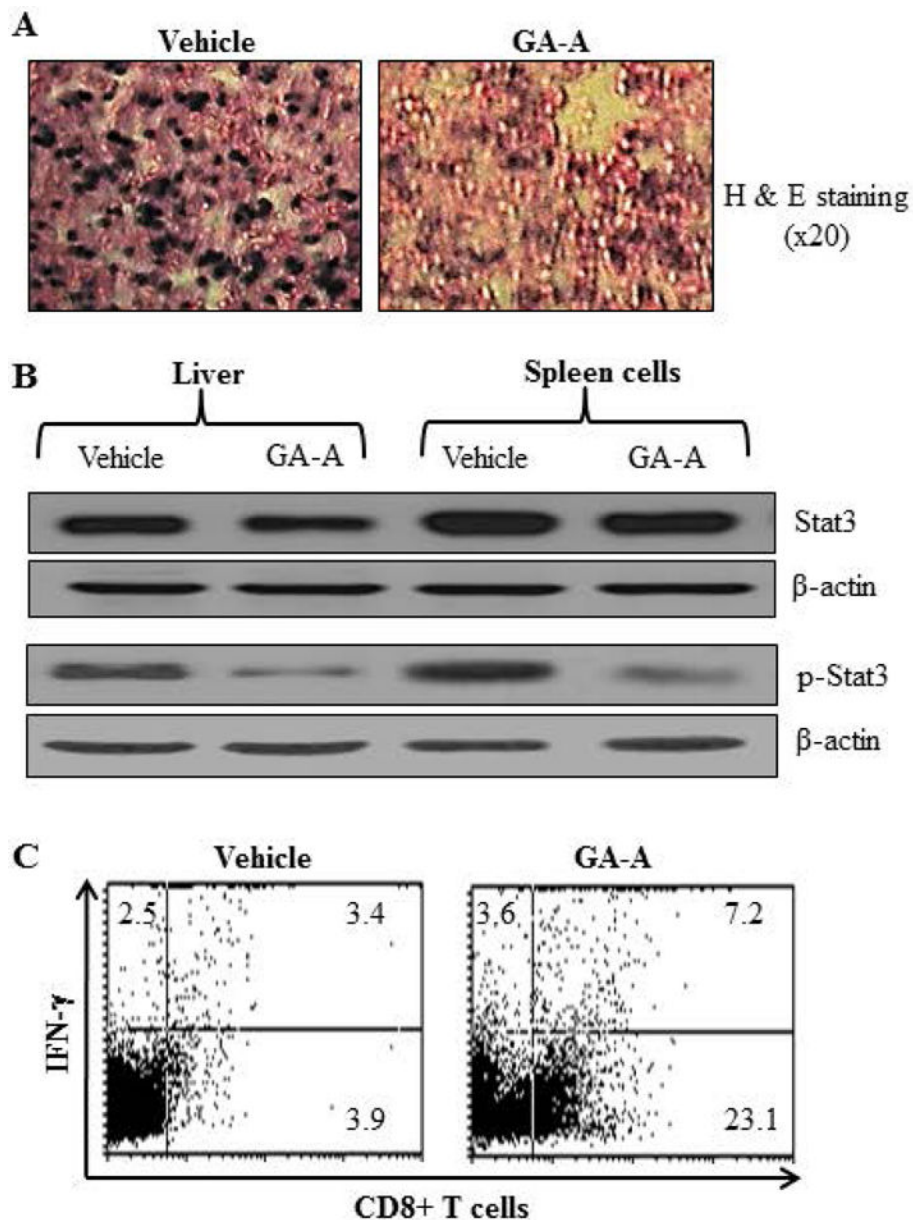
Fig. 7.
GA-A treatment activates cytotoxic CD8+ T cells and reduces EL4 metastatic lesions possibly via down-regulation of STAT3 phosphorylation. (A) Hematoxylin and Eosin staining of liver samples obtained from vehicle or GA-A treated EL4-bearing mice. Magnification, ×40. (B) Liver samples (pooled, n=3) as well spleen cells (pooled, n=3) obtained from vehicle and GA-A-treated mice were subjected to western blotting for analysis of STAT3 and p-STAT3 proteins. β-actin was used as a loading control. (C) Pooled spleen cells (pooled, n=3) from both groups were also washed and treated with 75ng/ml of PMA plus 300ng/ml of ionomycin, and were stained for 20min with FITC-labeled anti-CD8 monoclonal antibody as described in the methods. After washing twice, the cells were permeabilized (BD buffer) and stained for 30min at 4°C in the dark with PE-IFN-γ. Cells

were then analyzed by flow cytometry for CD8+ T cells and IFN-γ as described in the methods.